Lifetime of the 6793-keV State in ^{15}O

P. F. Bertone, A. E. Champagne, D. C. Powell, C. Iliadis, S. E. Hale, and V. Y. Hansper
The University of North Carolina at Chapel Hill, Chapel Hill, North Carolina 27599-3255
and Triangle Universities Nuclear Laboratory, Durham, North Carolina 27088-0308
(Received 5 February 2001; published 21 September 2001)

The energy derived from the CN cycle at low stellar temperatures is regulated by the ^{14}N$(p,\gamma)^{15}$O reaction. A previous direct measurement of this reaction has been interpreted as showing evidence for a subthreshold resonance which makes a major contribution to the reaction rate at low temperatures. This resonance, at $E_{\mathrm{c.m.}} = -504$ keV would correspond to the known $E_x = 6793$-keV state in ^{15}O. We have measured a mean lifetime of $1.60^{+0.75}_{-0.72}$ fs (90% C.L.) for this state using the Doppler-shift attenuation method. This lifetime is a factor of 15 longer than that inferred from the (p,γ) data and implies that the contribution of the subthreshold resonance is negligible.

DOI: 10.1103/PhysRevLett.87.152501 PACS numbers: 21.10.Tg, 26.20.+f, 27.20.+n, 97.10.Tk

Stars produce energy from the conversion of hydrogen into helium chiefly by the p-p chains and the CN cycle. The latter is the dominant source of energy for main-sequence stars with masses greater than about 1.5 times the mass of the sun, for all stars at the end of their main-sequence lifetimes, and on the red-giant branch. At the burning temperatures characteristic of these evolutionary stages ($T \approx 0.02$–0.08 GK or $T_9 \approx 0.02$–0.08), the ^{14}N$(p,\gamma)^{15}$O reaction is the slowest CN reaction and thus it regulates the rate of energy generation. Consequently, it impacts several areas of stellar structure and evolution. For example, the power liberated by the CN cycle and the amount of helium ash produced has a direct connection to the luminosity observed at the transition between the main sequence and the red-giant branch, and on the luminosity of the horizontal branch. The former is the primary tool for determining the ages of globular clusters [1]. The latter is one technique used to derive the distances to globular clusters and hence also plays a role in cluster ages [2,3]. In addition, the surface C/N ratio is an important diagnostic of the stellar interior [4] and this quantity is directly dependent (in part) on the ^{14}N$(p,\gamma)^{15}$O rate. Finally, since it helps to constrain the temperature and density profiles in the H-burning shell, ^{14}N$(p,\gamma)^{15}$O will affect nucleosynthesis beyond the CN cycle during the red-giant stage.

The thermonuclear reaction rate can be obtained from the astrophysical S factor, defined as

$$S(E_{\mathrm{c.m.}}) = E_{\mathrm{c.m.}}\sigma(E_{\mathrm{c.m.}})\exp(2\pi\eta), \qquad (1)$$

where $E_{\mathrm{c.m.}}$ is the energy in the center of mass, $\sigma(E_{\mathrm{c.m.}})$ is the reaction cross section, and η is the Sommerfeld parameter. The accepted S factor for the ^{14}N$(p,\gamma)^{15}$O reaction is based on the results of Schröder *et al.* [5] (hereafter SCH87). Their zero-energy S factor is $S(0) = 3.20(54)$ keV b and approximately half of this quantity is comprised of contributions from resonant (R) and direct-capture (DC) transitions to the ground state. The remainder derives from capture into the tail of a subthreshold resonance at $E_{\mathrm{c.m.}} = -504$ keV, corresponding to the known $E_x = 6793$-keV state in ^{15}O. The evidence for this particular contribution is inferred from the shapes of interference features in the $R/\mathrm{DC} \rightarrow$ ground-state channel of the (p,γ) excitation function. However, their fit to these data apparently did not include the tails of higher-energy resonances lying beyond the range of their measurement that could have produced similar interference effects at lower energies. Moreover, the width of the subthreshold state, $\Gamma = 6.3$ eV, is larger than what would be expected based on the width of the analogous state in ^{15}N ($\Gamma = 1.079$ eV). Although the isospin symmetry is not perfect, this level of disagreement is unexpected. In view of these potential uncertainties, a reevaluation of this reaction recommended $S(0) = 1.5$–4.5 keV b [6]. More recently, an R-matrix reanalysis of the data from SCH87 by Angulo and Descouvemont [7] resulted in $S(0) = 1.77 \pm 0.20$ keV b. Here, as in SCH87, the width of the subthreshold state was treated as a fit parameter.

The contribution of the -504-keV resonance can be estimated directly via a measurement of its mean lifetime. The technique that we have employed is the Doppler-shift attenuation method (DSAM), in which gamma rays are detected from a recoiling nucleus while it slows in a dense medium. The measured gamma-ray energy, E_γ, is then related to the emitted energy (in the center-of-mass frame), E_γ^0, via

$$E_\gamma = E_\gamma^0\left(1 + \frac{v_0}{c}F(\tau)Q\cos\theta\right), \qquad (2)$$

where v_0 is the initial recoil velocity, θ is the angle between the recoil direction and the emitted gamma ray, and Q is a (calculated) correction accounting for the finite size of the detector. The attenuation factor, $F(\tau)$, is related to the lifetime, τ, through [8]

$$F(\tau) = \frac{\int_0^\infty e^{-t/\tau}\overline{v(t)\cos(\phi)}\,dt}{v_0\tau}. \qquad (3)$$

Here $v(t)$ is the recoil velocity as a function of time and ϕ is the angular spread of the recoils. Both of these quantities can be predicted if the appropriate stopping powers can be calculated. However, in order to detect the attenuation of the Doppler shift, the recoiling nucleus must slow appreciably within a time comparable to the lifetime. In the present case, the lifetime expected from isospin symmetry is on the order of 1 fs and thus $F(\tau) \approx 1$. This regime requires both a heavy stopping medium and a low recoil velocity. Although the required sensitivity can be achieved in principle, difficulties can emerge in practice when the DSAM is applied to short lifetimes. For example, low recoil velocity implies that the observed energy shifts are small. In our experimental configuration, the full Doppler shift was 11 keV for gammas detected at 0^0. Consequently, it was necessary to determine the energy shift to better than 1 keV. We have made use of the first- and second-escape peaks in order to make three independent measurements of the energy shift at each detector angle (as will be discussed in more detail below). Another problem associated with low-energy recoils is that nuclear stopping becomes a major component of the total stopping power, and this is more difficult to calculate reliably than at higher energies where electronic stopping dominates. This in turn limits the accuracy of the lifetime that is extracted from $F(\tau)$. However, in this particular case we can make use of experimental constraints on the nuclear stopping. Thus, there are no fundamental limitations on the utility of the DSAM for such a short lifetime.

The $E_x = 6793$-keV state in ^{15}O was produced by the decay of the $E_{\mathrm{c.m.}} = 259$-keV resonance in $^{14}\mathrm{N}(p,\gamma)^{15}\mathrm{O}$. This resonance also populated the 5183- and 6176-keV states, which is important because the lifetime of the former state has been measured [9] and thus is used to check the reliability of the present measurement. The proton beam was provided by the TUNL minitandem accelerator [10]. This resonance was chosen because is satisfies the requirement of low recoil velocity (here corresponding to an energy of 18.6 keV or $\beta = 0.16\%$) and because its lifetime of 0.0066 fs [11] makes an insignificant contribution to our measured lifetimes. The target was produced by implanting ^{14}N into a thick tantalum substrate at an energy of 120 keV. The implanted dose (110 $\mu\mathrm{g/cm}^2$) was sufficient to produce a saturation density of ^{14}N. A measurement of the yield of the 259-keV resonance as a function of proton energy (Fig. 1), combined with the known resonance strength [11], yields a uniform profile with the Ta/N ratio of 0.72(11) on the plateau of the yield curve. This is in good agreement with 0.69(8) from previous studies [12]. In addition, the shape and width of the nitrogen profile are also consistent with previous measurements [13]. A beam energy of $E_p = 300$ keV was chosen to ensure that the reaction would occur well within the implanted layer. However, the short lifetime expected for the state of interest meant that the recoils would decay within the implanted region. Although the total stopping power here was somewhat less than that for pure Ta, the difference

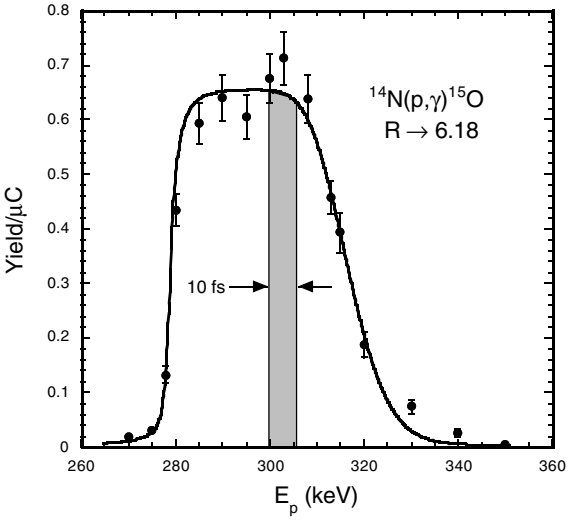

FIG. 1. $^{14}\mathrm{N}(p,\gamma)^{15}\mathrm{O}$ yield curve for the $E_{\mathrm{c.m.}} = 259$-keV resonance. The solid line is a fit to the data. The shaded area shows the region of the target (in energy units) traversed by an ^{15}O recoil in 10 fs, at a beam energy of 300 keV.

was small and had a negligible effect on our ability to determine $F(\tau)$.

Gamma rays were detected in three 60% HPGe detectors located at $\theta_{\mathrm{lab}} = 0°$, 90°, and 144° and at distances of 11 cm from the target. The gamma-ray spectra for each detector were calibrated independently using the known energies of lines from room background, sources, and the stopped component of the 6129-keV gamma-ray line produced by the $^{19}\mathrm{F}(p,\alpha_2\gamma)^{16}\mathrm{O}$ reaction at $E_p = 340$ keV. The average residuals of fits to the calibration lines were approximately 0.58 keV (90% C.L.). In addition, the residuals passed a T test at a 99% confidence level using a hypothesis of no energy dependence. Furthermore, the residuals for the escape peaks passed a one-sample T test at a 99% confidence level with the hypothesis that the average residual for the escape peaks was indistinguishable from that of the full-energy peaks. In other words, we could detect no systematic shift in the transition energy derived from a full-energy peak versus what was obtained using the escape peaks. Thus, our residuals provide a reasonable estimate of the calibration uncertainty, independent of energy. Also, at our level of uncertainty, there is no systematic trend in the $F(\tau)$ values derived from the escape peaks as compared to those obtained from the full-energy peaks.

Each of the 5183-, 6176-, and 6793-keV states decays directly to the ground state of ^{15}O. Portions of the spectra collected with the three detectors showing the full-energy peak for the $6793 \rightarrow 0$ transition are shown in Fig. 2. The energies of the first- and second-escape peaks and the full-energy peaks were used to make three independent determinations of $F(\tau)$, using Eq. (2). These values were then combined in a weighted average to yield $F(\tau) = 0.93(3)$ (90% C.L.). Our results are listed in Table I. The difference between our observed energy shift for the 6793-keV state and that expected for a full Doppler shift

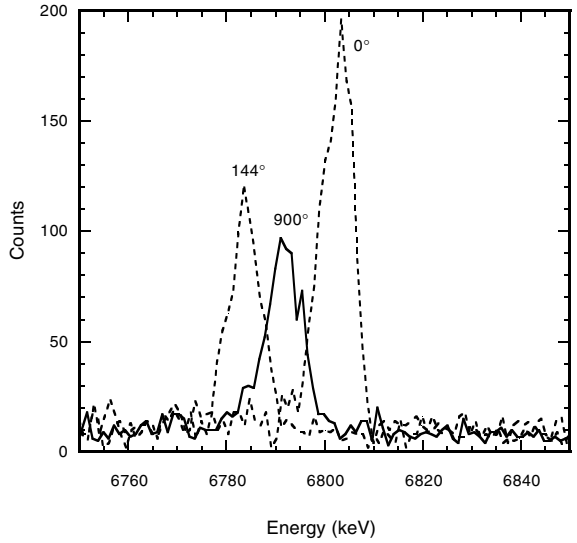

FIG. 2. Full-energy peaks for the $6793 \rightarrow 0$ transition, observed in the three Ge detectors.

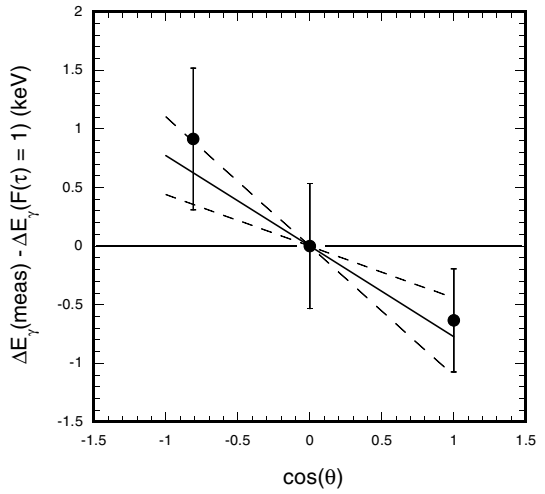

FIG. 3. Measured energy shift (defined as $E_\gamma - E_\gamma^0$) minus expected shift for $F(\tau) = 1$. For illustration, the solid line assumes $F(\tau) = 0.93$ and the dashed lines represent the 90% confidence range. Note that $F(\tau)$ was actually derived independently at each angle.

is shown in Fig. 3 as a function of $\cos(\theta)$. There is a significant difference between these two energy shifts.

Lifetimes were extracted from experimental values for $F(\tau)$ as described above, but assuming the Blaugrund approximation [14] in which the term $\overline{v(t)}\,\overline{\cos(\phi)}$ appearing in Eq. (3) is approximated by $v(t)\cos(\phi)$. This procedure is justified for our combination of short lifetime and dense stopping medium [14,15] and introduces a systematic uncertainty of about 5%–10% in the determination of τ. As a starting point, stopping powers were calculated with SRIM2000 [16] using our measured stoichiometry, assuming the density of Ta (16.4 g/cm^3 [17]). Although the implanted region is clearly not pure Ta, the differences in atomic size and electronegativity between Ta and N [17,18] suggest that N occupies interstitial, rather than substitutional, sites within the Ta lattice [19] and, therefore, the density should be close to that of Ta. This criterion is not exact [20], but does hold for N implanted into Ta [9]. Unfortunately, it is difficult to calculate low-energy stopping accurately. However, range distributions for 20–100 keV ^{15}N in Ta have been measured by Bister *et al.* [21], who conclude that the calculated nuclear stopping power should be corrected by a multiplicative factor 0.85(5). Similarly, they recommend that the electronic stopping power be multiplied by $1.0^{+0.4}_{-0.3}$. We have adopted these correction factors in the present work. The existence of this experimental constraint on the stopping power is important in that it limits what could be a large source of systematic uncertainty.

TABLE I. Experimental results.

E_x (keV)	$F(\tau)$	τ (fs) This study[a]	Literature[b]
5183	0.68(3)	$9.67^{+1.34}_{-1.24}$	8.2(10)
6176	0.91(5)	$2.10^{+1.33}_{-1.32}$	$\leq$2.5
6793	0.93(3)	$1.60^{+0.75}_{-0.72}$	$\leq$28, 0.1[c]

[a]The quoted uncertainties represent 90% confidence limits.
[b]Reference [11] unless otherwise noted.
[c]Reference [5].

The lifetime of the 6793-keV state is $\tau = 1.60^{+0.75}_{-0.72}$ fs (90% C.L.), where the uncertainties are purely statistical. In addition to random errors, there are also systematic uncertainties associated with the composition of the target (7.5% of τ), the calculation of stopping powers (5.1%), and the use of the Blaugrund approximation (about 5%–10%). Furthermore, our calculation of $F(\tau)$ ignores any spread in recoil energy or angle arising from the momentum carried by the primary gamma ray, but this effect contributes to the systematic uncertainty at a level of about 1%. Since it is difficult to estimate the uncertainty in target density, we have not included this source of systematic error. However, if the density of TaN is used (13.7 g/cm^3 [17]), then the lifetime would increase to 1.90 $\pm$ 0.87 fs, and in the extreme case, if the implanted nitrogen occupies substitutional lattice sites, then the density would be reduced to 7.6 g/cm^3 and τ would increase to 3.2 $\pm$ 1.5 fs. These values agree with our quoted results within statistical accuracy. As mentioned above, the measured lifetime of the 5183-keV state provides a means of assessing the reliability of our results. Our lifetime of $9.67^{+1.34}_{-1.24}$ fs (90% C.L.) is in good agreement with the previous value of 8.2(10) fs [9]. The earlier measurement also used the DSAM, but at higher recoil velocity where the corrections applied to the stopping powers have a smaller effect than in our case. In addition they used a thinner implanted layer of ^{14}N, which, when combined with the comparatively long lifetime of the 5183-keV state, meant that the recoils slowed in the Ta backing of their target. Therefore, their lifetime was less sensitive to uncertainties in target composition and density. Our agreement with this previous result indicates that our

target composition and density are accurate and that we have treated the stopping powers in a consistent fashion.

Our value for the lifetime of the 6793-keV state in ^{15}O is consistent with a total (observed) width of $0.41^{+0.34}_{-0.13}$ eV (90% C.L.) (at -504 keV), which is a factor of 15.4 smaller than the value implied by the S factor of SCH87. Consequently the contribution of this subthreshold resonance to the $R/\mathrm{DC} \rightarrow 0$ component of the $^{14}\mathrm{N}(p,\gamma)^{15}\mathrm{O}$ reaction rate is reduced by a similar amount. At low energies, the S factor for this transition is determined primarily by the net contribution of DC and the tail of the -504-keV resonances, with smaller contributions from higher-energy resonances. We have calculated $S(0)_{\mathrm{DC}} = 1.34$ keV b, using a spectroscopic factor $C^2S = 1.4$ [22] for the ground state. To calculate the tail of the subthreshold state, we have converted all widths to their formal values using a radius parameter of $r_0 = 1.25$ fm with $C^2S = 0.49$ [5] and a dimensionless reduced width of 0.79, as prescribed by Barker [23]. Using a one-level R-matrix approximation [24], we obtain $S(0) = 0.37^{+0.31}_{-0.12}$. This result *is* sensitive to the choice of the radius parameter. For example, varying r_0 from 1.12 to 1.45 fm changes $S(0)$ from 0.23 to 0.67 keV b. However, this will not have a large impact on the total reaction rate, as discussed below. The positive-energy resonances at 259, 987, and 2187 keV make small contributions (3.5×10^{-3}, 4.4×10^{-4}, and 0.018 keV b, respectively) to $S(0)$. The data of SCH87 indicate that the -504-keV resonance will interfere destructively with DC. Thus, the net S factor for $R/\mathrm{DC} \rightarrow 0$ at zero energy is $S(0) \approx 0.12-0.45$ keV b rather than 1.55 keV b quoted by SCH87. This is consistent with $S(0) = 0.08^{+0.13}_{-0.06}$ keV b as reported by Angulo and Descouvemont [7]. Our uncertainty range reflects our 90% C.L. values for the width of the subthreshold state, but ignores any uncertainties associated with the calculation of $S(0)$. The other channels in the $^{14}\mathrm{N}(p,\gamma)^{15}\mathrm{O}$ reaction contribute $S(0) = 1.65$ keV b. Therefore, for all channels, $S(0) \approx 2$ keV b, which is consistent with the lower limit advocated by Adelberger *et al.* [6] and with 1.77 ± 0.20 keV b from Angulo and Descouvemont [7].

With our new value for the lifetime of the 6793-keV state, the cross section for the direct transition to the ground state of ^{15}O is substantially reduced at low energies. Consequently, the major contributors to the reaction rate at low temperatures are the 259-keV resonance and DC to the 6793-keV state. The resulting rate is smaller than the value recommended by the NACRE Collaboration [25] for $T_9 < 0.2$. For example, the reduction for $T_9 = 0.02-0.1$ is 44%–34%. This leads to an increase in the age of the main-sequence turnoff in globular clusters by about 5% [3], assuming that the distance to the cluster is known. The luminosity of the horizontal branch will also be affected as will the ages derived using this quantity. However, this effect has not been examined in detail. There are larger consequences for studies of stellar structure and evolution. The interior conditions of model stars that produce energy via the CN cycle must be adjusted in order to produce the same outward pressure despite the increase in the CN cycle time. This could lead to enhancements in the predicted Na or Al abundance in massive stars [26]. Furthermore, the predicted surface C/N ratio will be modified. In CNO equilibrium, C/N is proportional to the rate of the $^{14}\mathrm{N}(p,\gamma)^{15}\mathrm{O}$ reaction and thus will be reduced *for a fixed temperature*. However, the predicted surface abundance could increase if the burning temperature increases to maintain the star in equilibrium. Detailed model calculations are under way to quantify these predictions [26].

This work was supported in part by USDOE Grant No. DE-FG02-97ER41041.

[1] D. A. VandenBerg, M. Bolte, and P. B. Stetson, Astron. J. **100**, 445 (1990).
[2] B. Chaboyer *et al.,* Science **271**, 957 (1996).
[3] B. Chaboyer *et al.,* Astrophys. J. **494**, 96 (1998).
[4] S. A. Becker and I. Iben, Astrophys. J. **232**, 831 (1979).
[5] U. Schröder *et al.,* Nucl. Phys. **A467**, 240 (1987).
[6] E. G. Adelberger *et al.,* Rev. Mod. Phys. **70**, 1265 (1998).
[7] C. Angulo and P. Descouvemont, Nucl. Phys. **A690**, 775 (2001).
[8] D. B. Fossan and E. K. Warburton, *Nuclear Spectroscopy and Reactions, Part C,* edited by J. Cerny (Academic Press, New York, 1974).
[9] J. Keinonen, M. Bister, and A. Anttila, Nucl. Phys. **A286**, 505 (1977).
[10] T. C. Black *et al.,* Nucl. Instrum. Methods Phys. Res., Sect. A **333**, 239 (1993).
[11] F. Ajzenberg-Selove, Nucl. Phys. **A523**, 1 (1991).
[12] J. Keinonen and A. Anttila, Nucl. Instrum. Methods **160**, 211 (1979).
[13] S. Seuthe *et al.,* Nucl. Instrum. Methods Phys. Res., Sect. A **260**, 33 (1987).
[14] A. E. Blaugrund, Nucl. Phys. **88**, 501 (1966).
[15] W. M. Currie, Nucl. Instrum. Methods **73**, 173 (1969).
[16] J. F. Ziegler and J. P. Biersack, program SRIM2000, 1999, (unpublished).
[17] *Handbook of Chemistry and Physics,* edited by D. R. Lide (CRC Press LLC, New York, 2000).
[18] S. Frage, K. M. S. Saxena, and J. Karwowski, *Handbook of Atomic Data* (Elsevier, New York, 1979).
[19] D. K. Sood, Phys. Lett. **68A**, 469 (1978).
[20] J. Keinonen *et al.,* Nucl. Instrum. Methods Phys. Res. **216**, 249 (1983).
[21] M. Bister, A. Anttila, and J. Keinonen, Phys. Rev. C **16**, 1303 (1977).
[22] S. V. Artemov *et al.,* Bull. Russ. Acad. Sci. Phys. **60**, 1816 (1996).
[23] F. C. Barker, Nucl. Phys. **A637**, 576 (1998).
[24] A. M. Lane and R. G. Thomas, Rev. Mod. Phys. **30**, 257 (1958).
[25] C. Angulo *et al.,* Nucl. Phys. **A656**, 3 (1999).
[26] M. F. El Eid, A. E. Champagne, and W. Shaya, *Nuclei in the Cosmos V, Proceedings of the International Symposium on Nuclear Astrophysics,* edited by N. Prantzos and S. Harissopulos (Editions Frontières, Paris, 1998), p. 123; M. F. El Eid (private communication).